Meson turbulence at quark deconfinement from AdS/CFT

Koji Hashimoto [a,b,∗], Shunichiro Kinoshita [c], Keiju Murata [d],
Takashi Oka [e]

[a] *Department of Physics, Osaka University, Toyonaka, Osaka 560-0043, Japan*
[b] *Mathematical Physics Lab., RIKEN Nishina Center, Saitama 351-0198, Japan*
[c] *Osaka City University, Advanced Mathematical Institute, Osaka 558-8585, Japan*
[d] *Keio University, 4-1-1 Hiyoshi, Yokohama 223-8521, Japan*
[e] *Department of Applied Physics, University of Tokyo, Tokyo 113-8656, Japan*

Abstract

Based on the QCD string picture at confining phase, we conjecture that the deconfinement transition always accompanies a condensation of higher meson resonances with a power-law behavior, "meson turbulence". We employ the AdS/CFT correspondence to calculate the meson turbulence for $\mathcal{N} = 2$ supersymmetric QCD at large N_c and at strong coupling limit, and find that the energy distribution to each meson level n scales as n^α with the universal scaling $\alpha = -5$. The universality is checked for various ways to attain the quark deconfinement: a static electric field below/around the critical value, a time-dependent electric field quench, and a time-dependent quark mass quench, all result in the turbulent meson condensation with the universal power $\alpha = -5$ around the deconfinement.

∗ Corresponding author.
  E-mail address: koji@phys.sci.osaka-u.ac.jp (K. Hashimoto).

1. Turbulence and quark deconfinement

How the quarks are confined at the vacuum of quantum chromodynamics (QCD) is one of the most fundamental questions in the standard model of particle physics. The question has attracted attention for long years, and recent investigations have diverse approaches. The question is difficult simply because of the fact that the confinement appears at the vacuum, not in a particular corner with specific external forces. Therefore, the confining vacuum can be broken in various manner as one departs from the vacuum with the help of some external forces. The forces include for example a finite temperature, a finite quark density and electric fields. Depending on how you break the vacuum confinement, the resultant deconfined phases show various aspects with various global symmetries. This variety makes the confinement problem even more difficult to be understood.

We would like to find a universal feature of the deconfinement. To understand the nature of the quark confinement, we need a proper observable which exhibits a universal behavior irrespective of how we break the confinement. In this paper, we propose a universal behavior of resonant mesons and name it *meson turbulence*.

As we have summarized in our letter [1], a particular behavior of resonant mesons (excited states of mesons) can be an indicator of the deconfinement. The meson turbulence is a power-law scaling of the resonant meson condensations. For the resonant meson level n ($n = 0, 1, 2, \ldots$), the condensation of the meson $\langle c_n(x, t) \rangle$ with its mass ω_n causes the n-th meson energy ε_n scaling as $(\omega_n)^\alpha$ with a constant power α. This coefficient α will be unique for a given theory, and does not depend on how one breaks the confinement. In particular, for the theory which we analyze in this paper, that is $\mathcal{N} = 2$ supersymmetric QCD with $\mathcal{N} = 4$ supersymmetric Yang–Mills as its gluon sector at large N_c at strong coupling, the universal power-law scaling parameter α is found to be

$$\langle \varepsilon_n \rangle \propto (\omega_n)^\alpha, \quad \alpha = -5, \tag{1}$$

where ε_n is the energy of the n-th meson resonance. Normally, for example at a finite temperature, the energy stored at the n-th level of the resonant meson should be a thermal distribution, $\varepsilon_n \propto \exp[-\omega_n/T]$. The thermal distribution is Maxwell–Boltzmann statistics, in which the higher (more massive) meson modes are exponentially suppressed. However, we conjecture that this standard exponential suppression will be replaced by a power-law near any kind of the deconfinement transitions. If we think of the meson resonant level n as a kind of internal momentum, then the energy flow to higher n can be regarded as a so-called weak turbulence. This is why we call the phenomenon meson turbulence, and the level n can be indeed regarded as a momentum in holographic direction in the AdS/CFT correspondence [2–4].

The reason we came to the universal power behavior is quite simple. We combined two well-known things,

- Mesons are excitations of an open QCD string.
  As is well known, mesons and their resonant spectra are described by a quark model with a confining potential. The confining potential has a physical picture of an open string whose end points are quarks. Rotating strings can reproduce Regge behavior of the meson resonant spectra.
- Deconfinement phase is described by a condensation of long strings.
  It has been argued that the deconfinement phase can be identified as a condensation of long QCD strings [7] (see [8–11]). Once long QCD strings are condensed in the background,
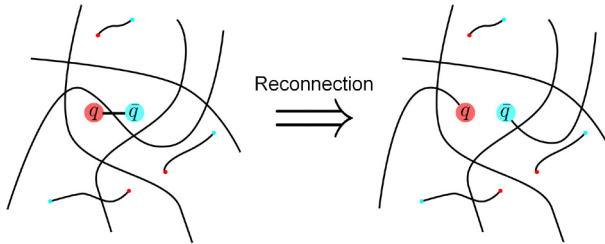
Fig. 1. A schematic picture of the deconfinement phase as condensation of QCD strings. Left: we add a meson (a pair of a quark and an antiquark connected by a QCD string) to the system. Right: due to the background condensed QCD strings, the QCD string can be reconnected, and the quark can freely propagate away from the antiquark.

if one adds a quark–antiquark pair to that, the string connecting the quark–antiquark pair can be reconnected with the background long QCD strings condensed, then the quark can propagate freely away from the antiquark. (See Fig. 1.) So the presence of the background QCD strings realizes the deconfinement. The picture is familiar in view of the renowned dual Meissner effect. Superconducting phase can be broken in a large magnetic field: many magnetic vortex strings are produced, and normal phase may be understood as condensed vortex strings. Upon the duality, the vortex strings correspond to the QCD strings, and confining (deconfining) phase corresponds to superconducting (normal) phase.

Combining these two leads us to the conjecture that *the deconfinement of quarks is indicated by a condensation of higher meson resonances*. More precisely, we claim that *the condensation should be turbulent*: the higher mode condensation is not suppressed exponentially but behaves with a power-law.

The reason we expect it to be a power law scaling is intuitively from a Hagedorn transition in string theory. String theory was born as an effective theory of hadrons at low energy, and is believed to be a good approximation at a large N_c limit of QCD. Since the number of states in string theory grows exponentially, a free string theory can reach an upper bound of the temperature which is called Hagedorn temperature. The exponential suppression of the higher states (Maxwell–Boltzmann statistics) is canceled by the growth of the number of states, and near the critical temperature the energy distribution changes from the exponential suppression law to a power-law.

The energy flow from larger scales to smaller scales with a universal power-law reminds us of turbulence in fluid dynamics. Indeed, the energy transfer between different scales because of non-linearities in some non-linear systems is called weak turbulence, and the Kolmogorov scaling factor $-5/3$ is universal in fluids. The name "meson turbulence" simply means that the energy distribution of the meson modes as a function of the meson resonant level n is the power-law with a universal power α. Here we regard the meson resonant level n as a kind of momentum, such that a larger n means a smaller scale. We are also motivated from a recent discovery of a weak turbulence in gravity in AdS, a Bizon–Rostworowski conjecture [12]. There, a power-law scaling of the energy distribution in the AdS gravity was found and is found to be universal for various initial conditions, indicating a turbulence. Since we shall work in the gauge/gravity correspondence, our meson turbulence may serve as a quark counterpart of the AdS instability.

In QCD, the phase transition region in the phase diagram is thought to be still at a strongly coupled regime, we in this paper employ the renowned AdS/CFT correspondence [2–4]. Since anyhow the AdS/CFT correspondence is expected to work well only at a large N_c limit which

is different from the realistic QCD, we use the most popular example in the AdS/CFT analysis: the $\mathcal{N} = 2$ supersymmetric QCD realized by the D3/D7 brane system [5]. Fortunately, the theory has a discrete meson states although the gluon sector is the $\mathcal{N} = 4$ supersymmetric Yang–Mills theory and thus is deconfined. We can concentrate on quark deconfinement, not the gluon deconfinement, in the model. The situation is somewhat similar to the heavy ion collision experiments as heavy quarkonia can survive even in the quark–gluon plasma.[1] In the AdS/CFT correspondence, there appears infinite number of meson resonances. They are just Fourier modes in holographic dimensions. So, higher meson resonant modes labeled by a large n corresponds to a smaller scale in the gravity dual, so our name "meson turbulence" can make sense in the gravity dual as a weak turbulence for the energy flow into a high frequency modes in extra holographic dimensions.

The meson turbulence is not the turbulence in the real space but in the holographic space, thus the power law is not of the real space momentum p but of the meson level n. The real-space turbulence in QCD has been studied in relation to thermalization at heavy ion collisions [14–25], based on general grounds for scalar/gauge field theories [26–35]. Note the difference from our turbulence in the holographic space.

We shall investigate various deconfining transitions in this paper, to check the universality of our conjecture of the meson turbulence. First, we work with a static case. A nonzero electric field is a good example since a strong electric field can make the quark–antiquark pair dissociate. Beyond the value of the electric field called Schwinger limit, the system experiences a phase transition from the insulator (confining) phase to a deconfined phase with electric quark current flow. We look at the situation just before/around the phase transition, and will find the meson turbulence.

Then we investigate time-dependent setup. The virtue of the AdS/CFT correspondence is that time-dependent analysis is possible, as opposed to lattice simulations of QCD. To demonstrate the universality of the meson turbulence, we work in two examples: (1) electric-field quench, and (2) quark-mass quench. In (1), we change the electric field in a time-dependent manner, from zero to a nonzero finite value, in a duration denoted by Δt. Then the system dynamically evolves and we follow it in the gravity dual of the gauge theory. At later times a singularity is formed, which signals the deconfinement [6]. We perform a spectral analysis of the mesons and find that, at high frequencies, the system is transferred from an initial spectrum determined by the quench to the power-law, with the universal coefficient $\alpha = -5$. Then in (2), we consider a time-dependent change in quark mass. The quark mass starts to grow and then comes back to the original value, in the duration Δt. In this case we will not include the worldvolume gauge field but excite only the brane fluctuations, because we attempt to explore the essence of the meson turbulence in the simplest setup. We again find the meson turbulence and the universal power law with the power $\alpha = -5$.

The universality we found in this paper strongly indicates that the meson turbulence is a universal phenomena which is independent of how one breaks the confinement. The condensation

---

[1] The $\mathcal{N} = 2$ supersymmetric QCD we consider has the $\mathcal{N} = 4$ sypersymmetric Yang–Mills theory as its gluon sector, and because of the maximal supersymmetries the color force is Coulombic. Nevertheless, at short distances the quark–antiquark potential is linear [13] (while at the large distances the potential is Coulombic). This strange behavior is due to the conformal property of the $\mathcal{N} = 4$ sector, and the theory does not have the asymptotic freedom. Thanks to this linear potential at short distances in the quark sector, the spectrum of the meson modes with low spins is linearly spaced. Our "quark deconfinement" refers to the disappearance of the linear potential due to the external forces such as the electric field. The disappearance is often called meson melting.

of long QCD strings in the completely deconfined phase is a difficult task, so we look into the behavior of mesons just before the deconfinement. We hope that our approach would serve as a new approach to understand the quark confinement problem.

The organization of this paper is as follows. First, we shall give a brief review of the holographic setup to introduce our notation, in particular, the meson effective action given by the AdS/CFT correspondence. Then in Section 3, we provide an analysis for the static case with the electric field. We illustrate the example with an evaluation of a vanishing string tension. In Section 4, we recall quenches in linear theory and examine non-linear evolutions of the electric field quench. In Section 5, we analyze the quark-mass quench as the simplest setup and demonstrate the universality of the meson turbulence. The final section is devoted to a summary.

2. Review: $\mathcal{N} = 2$ supersymmetric QCD in holography

The simplest set-up in string theory which accommodates quarks in four spacetime dimensions is the $\mathcal{N} = 2$ supersymmetric QCD. More precisely, the flavor quark sector is added as a kind of a probe and so the number of flavor is $N_f = 1$, while the gauge group is $U(N_c)$ with a large N_c limit, $N_c \to \infty$. The gluon part has the maximal supersymmetries, $\mathcal{N} = 4$. This set-up served as a best toy model of QCD in the AdS/CFT correspondence [5]. To obtain the gravity dual, we take the strong coupling limit $\lambda \equiv N_c g_{YM}^2 \to \infty$, too. Then the correspondence states that the meson sector is nothing but the flavor D7-brane action in the $AdS_5 \times S^5$ background geometry,

$$S = \frac{-1}{(2\pi)^6 g_{YM}^2 l_s^8} \int d^8\xi \sqrt{-\det(g_{ab}[w] + 2\pi l_s^2 F_{ab})},$$

$$ds^2 = \frac{r^2}{R^2}\eta_{\mu\nu}dx^\mu dx^\nu + \frac{R^2}{r^2}\left[d\rho^2 + \rho^2 d\Omega_3^2 + dw^2 + d\bar{w}^2\right], \tag{2}$$

where $r^2 \equiv \rho^2 + w^2 + \bar{w}^2$, $F_{ab} = \partial_a A_b - \partial_b A_a$, and $R \equiv (2\lambda)^{1/4} l_s$ is the AdS_5 curvature radius. The fields on the D7-brane, A_a and w, are on $(7 + 1)$-dimensional worldvolume.

We assume a trivial dependence on the internal direction within S^5 since they are expected to be irrelevant to the real QCD dynamics. Then the fields are dependent only on the AdS radial direction ρ and our $(3 + 1)$-dimensional spacetime, $w(x^\mu, \rho)$ and $A_a(x^\mu, \rho)$. Basically the decomposition of these five-dimensional fields into eigen-components in the ρ direction gives a Kaluza–Klein-like tower of infinite number of four-dimensional fields. The four-dimensional fields are the scalar and the vector mesons. So, the D7-brane action (2) is nothing but the meson effective action.

Let us write the meson decomposition and the effective action explicitly. A convenient rescaling for the vector field is $a_a \equiv 2\pi l_s^2 R^{-2} A_a$. Furthermore, we set $\bar{w}(x^\mu, \rho) = 0$ for simplicity. The theory has only a single scale which is the quark mass. It is defined by the location of the D7-brane at the asymptotic AdS boundary, as $w(x^\mu, \rho = \infty) = R^2 m$, where the quark mass m_q is given by this m as $m_q = (\lambda/2\pi^2)^{1/2} m$. The static solution of the shape of the D7-brane with this boundary condition at the AdS boundary is simply a straight D7-brane,

$$w(x^\mu, \rho) = R^2 m, \qquad a_a(x^\mu, \rho) = 0. \tag{3}$$

We consider a fluctuation of the fields around this background solution, and find a fluctuation action explicitly written to the second order in the fluctuation, as [13]

$$S = \int dt d^3x \int_0^1 dz \frac{1-z^2}{2z} [(\partial_t \boldsymbol{\chi})^2 - m^2(1-z^2)(\partial_z \boldsymbol{\chi})^2] + \mathcal{O}(\boldsymbol{\chi}^3),$$

where we have defined the fluctuation fields as $\boldsymbol{\chi} \equiv (R^{-2}w - m, a_x)$, and assumed that all fields are independent of the spatial coordinates x^1, x^2, x^3. Note that a_x denotes the vector field along an spatially-homogeneous direction in the Euclidean space with these coordinates. An irrelevant overall factor is neglected in the action. The new radial coordinate z is defined through

$$\rho \equiv R^2 m \frac{\sqrt{1-z^2}}{z}. \tag{4}$$

In this new coordinate, $z = 0$ is the AdS boundary, and $z = 1$ is the D7-brane center that is closest to the Poincaré horizon in the bulk AdS.

To calculate the meson modes, we solve the equation of motion for $\boldsymbol{\chi}$ to the leading order in the fluctuation,

$$\left[\frac{\partial^2}{\partial t^2} - m^2 \frac{z}{1-z^2} \frac{\partial}{\partial z} \frac{(1-z^2)^2}{z} \frac{\partial}{\partial z} \right] \boldsymbol{\chi} = 0. \tag{5}$$

This can be solved with

$$\boldsymbol{\chi} = \sum_{n=0}^{\infty} \text{Re} \left[C_n \exp[i\omega_n t] e_n(z) \right], \tag{6}$$

$$e_n(z) \equiv \sqrt{2(2n+3)(n+1)(n+2)} \, z^2 F(n+3, -n, 2; z^2), \tag{7}$$

where

$$\omega_n \equiv 2\sqrt{(n+1)(n+2)} \, m \tag{8}$$

is the resonant meson mass for the meson level number $n = 0, 1, 2, \ldots$, and F is the Gaussian hypergeometric function. Note that the resonant meson mass is almost equally spaced but not exactly.

The inner product in the z-space is defined as

$$(f, g) \equiv \int_0^1 dz \, z^{-1}(1-z^2) f(z) g(z), \tag{9}$$

with which the eigen-mode functions satisfy the ortho-normality condition

$$(e_n, e_m) = \delta_{mn}. \tag{10}$$

In particular, the eigen-functions $e_n(z)$ are normalizable. Note that an external electric field with $a_x = -Et$ satisfies Eq. (5) and it is non-normalizable, so giving a constant electric field background. Using the eigen-modes, to derive the meson effective action we expand the scalar field and the vector field as

$$\boldsymbol{\chi} = (0, -Et) + \sum_{n=0}^{\infty} c_n(t) e_n(z). \tag{11}$$

In this expansion, the coefficient fields $c_n(t)$ are meson fields, which share the same quantum charge. The non-negative integer n denotes the resonant level of the meson. The meson field

$c_n(t)$ corresponds to some quark bilinear operators such as $\bar{\psi}\psi$ and $\bar{\psi}\gamma_\mu\psi$, but there are important differences: First, the meson fields are fluctuation around the hadronic vacuum. So the value of the meson field, which is zero at the hadron vacuum, is not directly related to the operator expression, for example, $\langle\bar{\psi}\psi\rangle$ which is nonzero even at the hadron vacuum. Second, the normalization of the meson fields is determined such that the effective action of the meson has a canonically normalized kinetic term, so the relation to the operator expression is up to a normalization factor.

Substituting Eq. (11) back to Eq. (2), we obtain the meson effective action

$$S = \frac{1}{2}\int d^4x \sum_{n=0}^{\infty}\left[\dot{c}_n^2 - \omega_n^2 c_n^2\right] + \text{interaction}, \tag{12}$$

where we have omitted a constant term and total derivative terms. One can work out all the nonlinear interaction terms if one wishes. We can define the energy stored in the n-th meson resonance as

$$\varepsilon_n \equiv \frac{1}{2}(\dot{c}_n^2 + \omega_n^2 c_n^2) \tag{13}$$

and also the linearized total energy

$$\varepsilon = \sum_{n=0}^{\infty}\varepsilon_n. \tag{14}$$

These expressions for the meson energies will be used later for evaluating how much energy is stored to the level n meson resonance.

The important term is the interaction terms in the meson effective action. They make an energy transfer from one level to another. We need not to explicitly calculate the interaction terms in terms of the component meson resonant fields. In the following sections, we use the D7-brane action itself to calculate the scalar/vector fields in a time-dependent manner, and then decompose the fields into the meson resonances by using the inner-product and the ortho-normality (10).

3. Meson turbulence at static electric field

3.1. Bending of the D7-brane

In this section, we shall evaluate the turbulent meson condensation for a deconfinement caused by a static and constant electric field. We first solve the shape of the D7-brane for the finite electric field, and decompose the scalar field into the meson resonance.

But before considering the electric field, it would be instructive to consider the case with a finite temperature, as a warm-up example to grasp what will happen to the probe D7-brane around the deconfinement transition. Once we turn on a temperature, the background geometry of AdS_5 starts to deform and has a horizon. The D7-brane starts to be deformed, see Fig. 2. This deformation is due to a supersymmetry breaking by the black hole horizon (or by the temperature). The central part of the D7-brane is attracted to the black hole horizon, and finally is absorbed into the horizon. The D7-brane before hitting the black hole horizon is called "Minkowski embedding", while the D7-brane whose tip is already inside the horizon is called "black hole embedding". When a part of the D7-brane is inside the horizon, the spectrum of the fields on the D7-brane becomes continuous, which means that the mesons melt and we are at a deconfined phase. So, hitting the black hole horizon is the deconfinement transition.
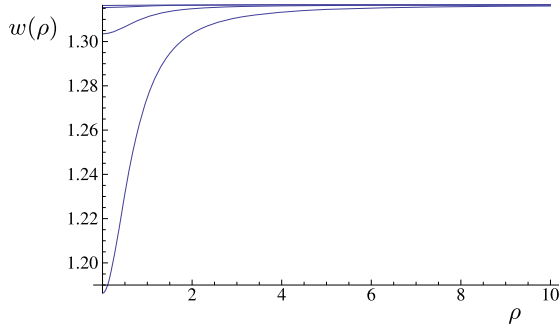
Fig. 2. The shape of the D7-brane in the AdS Schwarzschild background. As the temperature of the background geometry increases, the shape changes and the D7-brane bends toward the black hole.
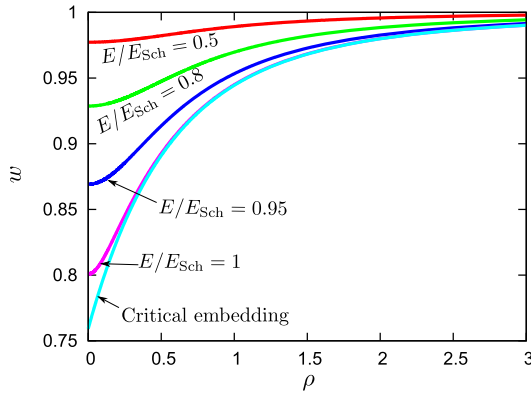

Fig. 3. The shape of the probe D7-brane in static electric fields in the unit of $R = m = 1$. The lines correspond respectively to $E/E_{\mathrm{Sch}} = 0.5, 0.8, 0.95, 1$ and the critical embedding from top to bottom.

From Fig. 2 we can see that the D7-brane gets sharper and sharper as we increase the temperature. And in fact, at the deconfinement transition, the D7-brane needs to be conical if we assume that the deformation is smooth. This is because at the black hole horizon the redshift factor is infinite, so anything should be perpendicular to the horizon. In order to have this conical shape, we need to turn on higher resonant modes of mesons, since the mode (resonant level) number is almost like a Fourier level. This basically tells us that the deconfinement transition is accompanied with higher resonant meson condensation, that is, the turbulent meson condensation.

Now we proceed to the case with a finite electric field on the D7-brane. In fact, the situation is quite similar to the case of the finite temperature black hole in the background. First, let us look at the D7-brane shape with the finite electric field on the D7-brane, see Fig. 3. It is a plot of the solution of the equations of motion of the D7-brane action (2) with the electric field is introduced by a solution $a_x = -Et$. The calculation was originally performed in Refs. [36–38]. The shape has a similar structure to the case of the finite temperature. As we increase the electric field E, the D7-brane bends toward the Poincaré horizon of the AdS geometry.

Fig. 3 is with various value of the electric field in the unit of the Schwinger limit $E = E_{\mathrm{Sch}} = 0.5759m^2$ (in the unit $R = 1$). Beyond the Schwinger limit of the electric field, a first order phase transition to deconfinement occurs [37,38]. In Fig. 3, we also plot the case with a critical embedding. At the critical embedding, the bending of the D7-brane is the sharpest. The critical
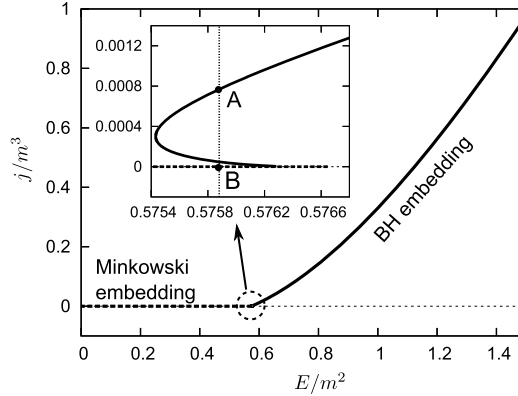
Fig. 4. The electric current j as a function of the electric field E. At the line AB, the phase transition occurs where $E = E_{\text{Sch}}$. The transition is the formation of an effective horizon of the world volume of the D7-brane. The D7-brane configuration exists even beyond $E = E_{\text{Sch}}$, and the largest E with the Minkowski embedding is called critical embedding which is the phase boundary between the Minkowski and black hole embeddings.

embedding is a boundary of the Minkowski embedding and the black hole embedding, and is not favored thermodynamically, see the phase diagram of the electric field E versus the electric current j, Fig. 4. At point AB (the Schwinger limit) the phase transition occurs, but the Minkowski embedding is possible even beyond $E = E_{\text{Sch}}$. The end point to the right of the point B is the critical embedding. The importance of the critical embedding is that it is a phase boundary and reflects the information of the black hole embedding most. At the critical embedding, the brane shape is conical.

3.2. Turbulent meson condensation

Let us examine the meson condensation for each resonant mode. We have learned that at the critical embedding which is the phase boundary to the black hole embedding the D7-brane's shape is conical. Once the brane is conical, it needs a condensation of infinitely high Fourier modes. This signals the turbulent meson condensation.

To look at how each meson behaves as we approach the critical embedding, we decompose the solution (shape) $\chi(t, z)$ of the D7-brane action (2) into the meson resonant modes, Eq. (11). The result is shown in Fig. 5. There we plot the ratio $|c_n|/|c_0|$ as a function of n where we define $|c_n| \equiv \sqrt{(c_n^{\text{scalar}})^2 + (c_n^{\text{vector}})^2}$ for illustration. We find two facts:

- As we increase the electric field, the condensation of the high resonant modes ($c_n, n \gg 1$) get more enhanced.
- At the critical embedding, the higher resonant modes participate stronger than the Maxwell–Boltzmann law.

Whether the Maxwell–Boltzmann law is replaced by the power-law or not can be seen clearly when the energy deposit to each meson is measured as a function of the meson resonance mass ω_n. For the static solutions, the energy expression (13) is simplified just to $\varepsilon_n = \omega_n^2 c_n^2/2$. In Fig. 6, we plot the meson energy distribution as a function of the resonant meson level n. In
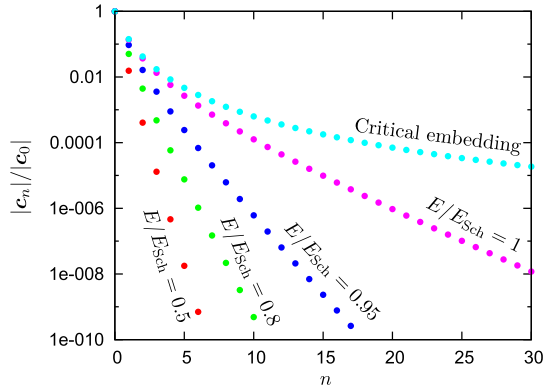
Fig. 5. Decomposed meson condensate $\log[|c_n|/|c_0|]$ in static electric fields. Colors red/green/blue/magenta/cyan correspond respectively to $E/E_{\text{Sch}} = 0.5, 0.8, 0.95, 1$ and the critical embedding. (For interpretation of the references to color in this figure, the reader is referred to the web version of this article.)
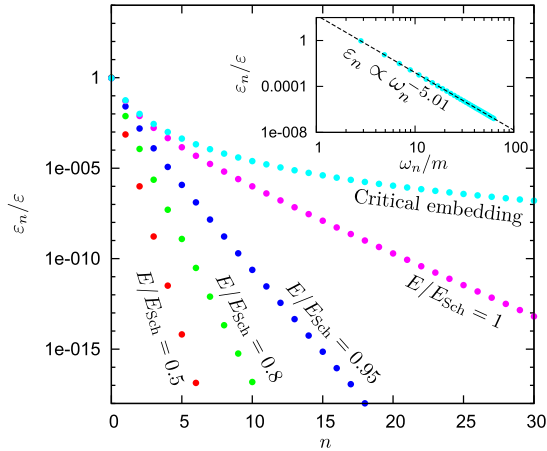

Fig. 6. The energy distribution for the n-th meson resonance. The color of the dots follows that of the previous figure. The inset is the log–log plot of the energy distribution for the critical embedding, in which we take the meson mass spectrum ω_n as the horizontal axis.

the upper-right corner of Fig. 6, we have a log–log plot and find a power-law distribution of the energy,

$$\varepsilon_n \propto \omega_n^{-5.01}. \tag{15}$$

Thus the power is found to be $\alpha = -5.01$. This shows a clear result of the turbulent meson condensation. The scaling of the energy as a function of the meson level n (which is a holographic momentum quantized) reminds us of a Kolmogorov scaling of turbulence.

We conclude that for the static case with a constant electric field, right before the quark deconfinement transition the meson resonances condense coherently and in a turbulent manner.

We have several comments. First, in our static example of the constant electric field, we have no condensation of the vector mesons. This is consistent: only mesons which possess the same quantum number as the vacuum get condensed, and no further symmetry breaking occurs at

the deconfinement transition. Second, how can we see the turbulent condensation in the meson theory? Our meson effective action (12) includes various couplings and coefficients, which are dependent on the electric field. Once we increase the electric field, the coefficient changes, and the mesons start to get condensed. Mesons in a theory with a single flavor is neutral under the electric field, but the meson can polarize and has a nonlinear dependence in E. In particular, in this theory exists a one-point function of the scalar mesons for a nonzero E, which drives the meson condensation.

3.3. Relevance to the string condensation

So far, we have considered only the scalar and the vector fields on the D7-brane. these are massless excitations of an open string on the D7-brane. The infinite tower of the meson resonances which we saw above is just a Kaluza–Klein-like tower obtained by a decomposition in the radial holographic direction. So, intuitively, they do not directly correspond to the long QCD strings. This seems to be unsatisfactory for our purpose, since our power-law conjecture came from the intuitive picture of the deconfined phase that is a condensation of long strings.

To fill this gap, we consider an open string attached to the D7-brane, see Fig. 7. The tension of the open fundamental string at the tip of the D7-brane is nothing but the Regge slope, thus is an effective QCD string tension of the theory. Now, as we turn on the electric field, the D7-brane shape changes and the effective tension changes. In addition, since the electric field pulls the ends of the open string (quarks) directly, thus makes the effective QCD string tension reduce. We shall see that the effective QCD string goes to zero near the deconfinement transition.

The open string tension at the tip of the D7-brane is given by

$$\sigma_{st} = \frac{1}{2\pi l_s^2} \sqrt{-g_{00}g_{11}} - \frac{R^2}{2\pi l_s^2} E . \tag{16}$$

The open string worldsheet is put along the direction of the electric field. The last term is the subtraction due to the electric field for giving the effective QCD string tension. The metric in the Nambu–Goto action should be evaluated at the tip of the D7-brane $w(\rho = 0)$, so

$$\sigma_{st} = \frac{1}{2\pi l_s^2} \left[\frac{w(\rho = 0)^2}{R^2} - R^2 E \right] . \tag{17}$$

Since we know how the tip of the D7-brane $w(\rho = 0)$ depends on the electric field E, we can numerically evaluate the tension σ_{st}. The result is shown in Fig. 8. We find that the effective QCD string tension goes to zero near the deconfinement transition. So, we conclude that not only the higher meson resonance from the massless open string modes but also the whole string excitations get condensed at the deconfinement transition.

Generically, when the D-brane action density vanishes due to the electric field, the electric field value is equal to the open string tension at the point of the vanishing D-brane action density [41–43]. When the D-brane action density vanishes, the system is expected to undergo a phase transition to the deconfined phase, and our finding is consistent. Furthermore, the vanishing tension of the QCD string at the deconfinement transition is consistent with the lattice data on entropy of a heavy quark pair [44].

The string condensation shows up in string theory at finite temperature. The Hagedorn transition is related to a condensation of strings winding the temporal direction [39,40]. In our present case, the deformed D7-brane serves as a probe of a horizon, and we can see the tendency to the
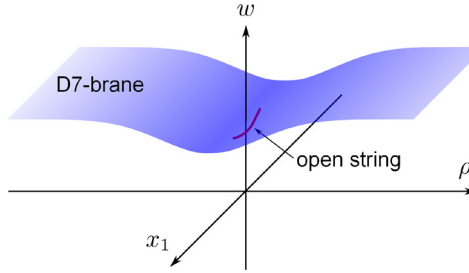
Fig. 7. The configuration of a fundamental string. The mesons are excited states of a fundamental open string hanging from the D7-brane. Lower excitations correspond to short string, which becomes almost parallel to the worldvolume of the D7-brane.
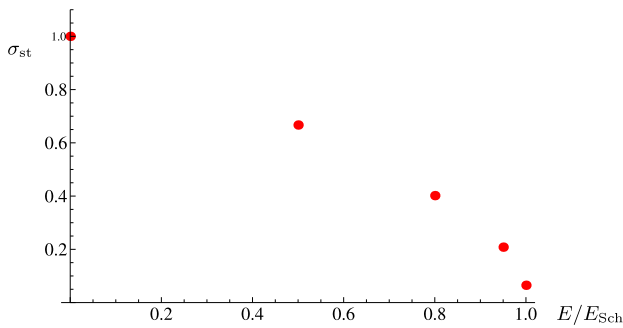

Fig. 8. The string tension $\sigma_{st}(E)$ in the unit of $\sqrt{2\lambda}m^2/2\pi$. Increase of the electric field makes the effective string tension decrease. The string tension approaches zero near the phase transition.

condensation by approaching the phase transition gradually (see [45] for a discussion on how the horizon can be seen as a Hagedorn transition).

The vanishing of the D-brane action mimics a tachyon condensation in string theory. When an electric field is present at the tachyon condensation, string fluid appears [46–48]. The string fluid is a macroscopic fundamental strings, and is similar to the background QCD string in spirit. Furthermore, when the electric field becomes critical, the original D-brane seems to lose the property with the vanishing tension and can be of arbitrary shape; a supersymmetric example is a super tube [49]. In this way, the vanishing D-brane action density provides universally a condensation of macroscopic strings, and through the AdS/CFT correspondence they correspond to the QCD strings. Our example supports the generic feature of the D-branes at criticality.

4. Meson turbulence in quenched electric fields

Now, we shall turn to the meson turbulence in time-dependent set-up. The higher meson condensation seems to be a sufficient cause of quark deconfinement. In this section, this is clearly seen in a time-dependent, electric field quench that we study below.

4.1. Linear theory for quenches

Before we discuss non-linear time-evolutions in the electric field quench, let us recall linear theory regarding quenches as perturbations. This linear analysis is also available for the quark-

mass quench which will be studied in the next section. By comparing analytic results of the linear analysis with the following numerical non-linear evolutions, we can clarify when the non-linearity will significantly affect dynamics on the brane. Then, it turns out that the linear analysis is useful for considering initial spectrum of excitations caused by the quenches.

The equation of motion for the fluctuations χ is

$$\left[\frac{\partial^2}{\partial t^2} - m^2 \frac{z}{1-z^2} \frac{\partial}{\partial z} \frac{(1-z^2)^2}{z} \frac{\partial}{\partial z} \right] \chi = 0, \tag{18}$$

where χ can describe both fluctuations of the brane position and the worldvolume gauge field, namely $\chi = (W - m, a_x)$. Note that we can deal with the both fluctuations identically because mass spectra of the scalar and vector mesons corresponding to the fluctuations of scalar and gauge fields respectively are degenerate in absence of the static electric field.

The Fourier transform of a solution χ is

$$\hat{\chi}(\omega, y) = \frac{1}{2\pi} \int_{-\infty}^{\infty} \chi(t, z) e^{-i\omega t} dt, \tag{19}$$

and satisfies the differential equation

$$y(1-y)\hat{\chi}'' - 2y\hat{\chi}' + \frac{\omega^2}{4m^2}\hat{\chi} = 0, \tag{20}$$

where $y \equiv z^2$ and the prime denotes y-derivative. Imposing boundary conditions that χ is regular at the pole ($y = 1$) and satisfies $\chi(t, 0) = \chi_0(t)$ at the AdS boundary ($y = 0$), we have

$$\hat{\chi}(\omega, y) = \hat{\chi}_0(\omega) \frac{F(\lambda_+, \lambda_-, 2; 1-y)}{F(\lambda_+, \lambda_-, 2; 1)}, \tag{21}$$

where $\lambda_\pm(\omega) = (1 \pm \sqrt{1 + \omega^2/m^2})/2$ and $\chi_0(t) = \int_{-\infty}^{\infty} \hat{\chi}_0(\omega) e^{i\omega t} d\omega$. The function $\chi_0(t)$, which is assumed to be $\chi_0(t) = 0$ for $t < 0$, gives us mass or electric field quench at the boundary. Here, the latter fractional part of Eq. (21) has no pole in the lower half-plane of ω, because it is nothing but a Fourier transform of a response function. Note that

$$F(\lambda_+, \lambda_-, 2; 1) = -\frac{4m^2}{\pi\omega^2} \cos\left(\frac{\pi}{2}\sqrt{1 + \omega^2/m^2} \right). \tag{22}$$

Using the following formula

$$\frac{\pi}{\cos \pi x} = -\sum_{n=0}^{\infty} \frac{(-1)^n (2n+1)}{x^2 - (n + \frac{1}{2})^2}, \tag{23}$$

we can rewrite (21) as

$$\hat{\chi}(\omega, y) = \hat{\chi}_0(\omega) \sum_{n=0}^{\infty} \frac{(-1)^n (2n+1)\omega^2}{\omega^2 - 4n(n+1)m^2} F(\lambda_+, \lambda_-, 2; 1-y)$$

$$= \hat{\chi}_0(\omega) \left[1 - \sum_{n=0}^{\infty} \frac{(-1)^n (2n+3)\omega^2}{\omega^2 - 4(n+1)(n+2)m^2} \right] F(\lambda_+, \lambda_-, 2; 1-y), \tag{24}$$

where in the square bracket the former term is the non-normalizable mode and the latter term is a summation of the normalizable modes with poles representing the meson masses.

In the time domain, the normalizable part of the solution after the quench $t > 0$ becomes

$$
\chi(t, z) - \chi_{\text{non}}(t, z) = -\sum_{n=0}^{\infty} \int_{-\infty}^{\infty} d\omega e^{i\omega t} \frac{(-1)^n (2n+3)\omega^2}{(\omega - i0^+)^2 - \omega_n^2} F(\lambda_+, \lambda_-, 2; 1 - z^2) \hat{\chi}_0(\omega)
$$

$$
= 2\pi i \sum_{n=0}^{\infty} \frac{2n+3}{2} \omega_n z^2 F(n+3, -n, 2; z^2) e^{i\omega_n t} \hat{\chi}_0(\omega_n) + \text{c.c.}
$$

$$
= 2\pi i m \sum_{n=0}^{\infty} \sqrt{\frac{2n+3}{2}} \hat{\chi}_0(\omega_n) e^{i\omega_n t} e_n(z) + \text{c.c.,} \tag{25}
$$

where we have used $F(\lambda_+, \lambda_-, 2; 1 - z^2)|_{\omega=\omega_n} = (-1)^n z^2 F(n+3, -n, 2, z^2)$. The eigen-functions $e_n(z)$ and the eigen-value ω_n have been defined by (7) and (8), respectively. Note that $\chi_{\text{non}}(t, z)$ is the non-normalizable mode.

As a result, in linear response the quench characterized by the boundary condition $\chi_0(t)$ will cause excitations with the energy spectrum

$$
\varepsilon_n \equiv \frac{1}{2}(\dot{c}_n^2 + \omega_n^2 c_n^2) = 4\pi^2 m \omega_n^2 \sqrt{\omega_n^2 + m^2} |\hat{\chi}_0(\omega_n)|^2, \tag{26}
$$

where $\chi(t, z) = \chi_{\text{non}}(t, z) + \sum_{n=0}^{\infty} c_n(t) e_n(z)$.

4.2. Energy transfer to higher meson modes

Now, we consider the electric field quench in full non-linear theory. Assuming translational symmetry generated by $\partial_{\vec{x}}$ and spherical symmetry of S^3, we can write the dynamical brane solution as

$$
w = W(t, \rho), \quad 2\pi \ell_s^2 L^{-2} A_x = a_x(t, \rho), \tag{27}
$$

where we set $\bar{w} = 0$ without loss of generality.

We consider a time-dependent boundary condition for a_x as

$$
a_x|_{\rho=\infty} = -\int dt\, E(t), \tag{28}
$$

where $E(t)$ corresponds to the external electric field in the boundary theory $\mathcal{E}(t)$ as $\mathcal{E} = (\lambda/(2\pi^2))^{1/2} E$. Starting from the $E = 0$ vacuum in the confined phase $W = m$ for $t < 0$, we turn on the electric field smoothly to reach a final value E_f in the duration Δt. Explicitly, we choose a C^2 function for $E(t)$ as

$$
E(t) = \begin{cases} 0 & (t < 0) \\ E_f[t - \frac{\Delta t}{2\pi} \sin(2\pi t/\Delta t)]/\Delta t & (0 \le t \le \Delta t) \\ E_f & (t > \Delta t) \end{cases} \tag{29}
$$

The profile of the electric field is shown in Fig. 9. In our previous work [6], we solved the brane motion numerically imposing the boundary condition (28).[2] When the final value of the electric

---

[2] In [6], we used the in-going Eddington–Finkelstein time $V \equiv t - 1/r$ as the bulk time coordinate for the convenience of numerical calculations. At the AdS boundary $r = \infty$, both time coordinates V and t mean the same boundary time.
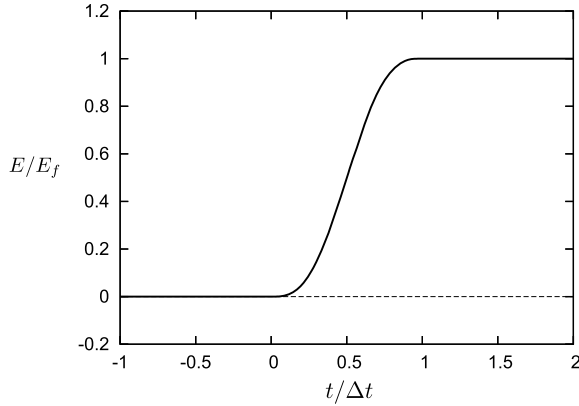
Fig. 9. Profile of the time-dependent electric field $E(t)$.

field E_f is below the Schwinger limit E_{Sch}, at which deconfinement transition occurs, a pulse-like fluctuation induced by the electric field quench at the AdS boundary propagates between the AdS boundary ($\rho = \infty$) and the pole ($\rho = 0$) on the brane worldvolume. We found that, after several bounces, the fluctuation collapses to a naked singularity at $\rho = 0$ depending on parameters E_f and Δt. It turns out a strongly redshifted region appears near the naked singularity. This is interpreted as an "instability" toward deconfinement, which happens, to our surprise, even when the final field strength is below the Schwinger limit.

Our finding can be considered as a probe-brane version of the weakly turbulence similar to that of the global AdS spacetime [12] in which a non-linear evolution of a perturbed AdS space-time causes an instability resulting in a black hole formation. They studied the energy spectrum of the perturbation and found that the energy is transferred from low to high frequencies as time increases. Following them, we also study the time evolution of energy spectrum of the brane fluc-tuation in spectral analysis. In the following, we choose a weak electric field ($E_f/E_{\text{Sch}} = 0.2672$) and a switch-on duration $m\Delta t = 2$, in which sub-Schwinger-limit deconfinement is realized. We decompose the time-dependent non-linear solutions obtained in Ref. [6] into normal modes, Eq. (7), on the supersymmetric background and calculate the condensate c_n and energy spectrum ε_n of the meson resonances. In Fig. 10(a), the time evolution of the condensate $|c_n|$ is shown for several time slices $mt = 10, 40$, and 49.3, while the time $mt = 49.3$ is just before deconfinement. Also, that of the energy spectrum $\varepsilon_n/\varepsilon$ is shown in Fig. 10(b).

In linear theory, from Eq. (26), we obtain the energy spectrum analytically as

$$
\begin{aligned}
\varepsilon_n^{\text{linear}} &= 4\pi^2 m \sqrt{\omega_n^2 + m^2} |\hat{E}(\omega_n)|^2 \\
&= \frac{32\pi^4 E_f^2 m \sqrt{\omega_n^2 + m^2}(1 - \cos \omega_n \Delta t)}{\omega_n^4 \Delta t^2 (4\pi^2 - \omega_n^2 \Delta t^2)^2},
\end{aligned}
\tag{30}
$$

where we have used $\hat{\chi}_0(\omega) = i\hat{E}(\omega)/\omega$ and $\hat{E}(\omega) = (2\pi)^{-1} \int_{-\infty}^{\infty} E(t)e^{-i\omega t} dt$ for the electric quench. We show the $\varepsilon_n^{\text{linear}}$ in Fig. 10(b) regarding ω_n as a continuous number for visibility. For a large n, the spectrum in linear theory becomes $\varepsilon_n^{\text{linear}} \propto (1 - \cos \omega_n \Delta t)/\omega_n^7$. Because of the trigonometric function $\cos \omega_n \Delta t$, it oscillates as a function of ω_n. We find that at an early stage of the time evolution the energy spectrum can be very well described by that of the liner theory $\varepsilon_n^{\text{linear}}$, and then gradually evolves as the condensate and the energy are transferred to
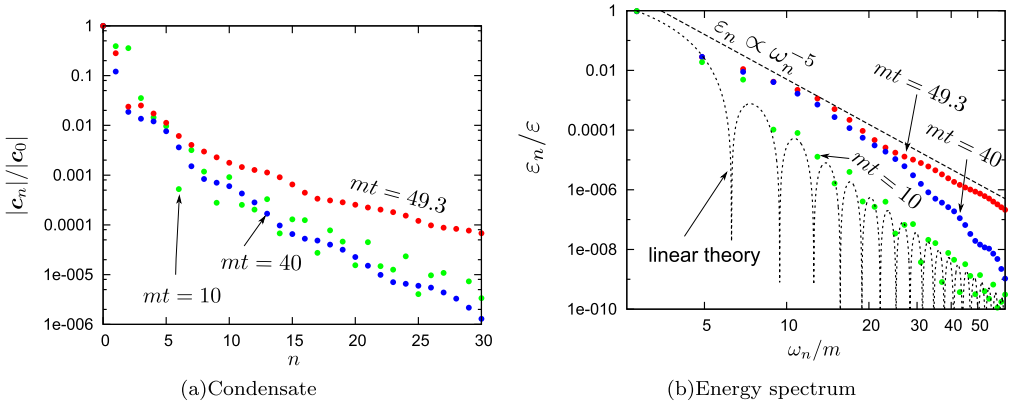
Fig. 10. (a) Condensate and (b) energy contributed by n-th exited meson induced by an electric field quench. Data for times $mt = 10$, 40, and 49.3 are shown. We set $E_f/E_{\mathrm{Sch}} = 0.2672$ and $m\Delta t = 2$. A clear (non-thermal) growth at large n is found along the time evolution. The energy spectrum agrees with that of the linear theory initially and then seems to approach $\varepsilon_n \propto \omega_n^{-5}$ as time increases.

higher meson modes during the time evolution. This tendency is similar to the static case in which they are "transferred" more as electric fields are stronger. Eventually, the energy spectrum $\varepsilon_n/\varepsilon$ seems to approach $\varepsilon_n \propto \omega_n^{-5}$ just before the deconfinement, which has been seen in the static calculation. (See Fig. 6.) It reminds us a Kolmogorov-like scaling again. This indicates that higher meson condensation is universally related to quark confinement.

The observed time evolution of the distribution suggests that turbulence is taking place in the meson sector. This is because higher modes have smaller wave lengths in holographic directions, and the transfer of energy and momentum indicates that smaller structure are being organized during the time evolution toward deconfinement.

4.3. Condition for the turbulent meson condensation

In Ref. [12], it was suggested that the global AdS is unstable against the black hole formation even for arbitrary small perturbations (see also [50]). Here, we explore the condition for the singularity formation in the D3/D7 system with the external electric field (29). In our previous work [6], we introduced the redshift factor $r_s(P_1, P_2) \equiv \omega(P_2)/\omega(P_1)$ associated with an outgoing light ray connecting between P_1 and P_2, where P_1 and P_2 are points at the initial surface and the AdS boundary, respectively. $\omega(P_1)$ and $\omega(P_2)$ are frequencies of the light ray measured by natural static observes at each point. Using the redshift factor, we defined the deconfinement phase in the view of the gravity side: we say the point P_2 of the boundary is in deconfinement phase when $r_s(P_1, P_2)$ has been very large (we use $r_s = 100$ as a criterion). We also defined the deconfinement time t_d which is the boundary time at which $r_s = 100$ is satisfied. In Ref. [6], we found that the redshift factor suddenly increases around a retarded time at which the singularity is formed. As a result, it exceeds our criterion of the deconfinement $r = 100$, and eventually it diverges. So, the deconfinement time t_d can be a good indication of the singularity formation. If there exists any non-zero minimum value of E_f as $t_d \to \infty$, the singularity formation does not occur for arbitrary small E_f. We will seek such a threshold value of E_f in the following.

In Fig. 11, we plot the inverse of the deconfinement time $1/(mt_d)$. Note that the deconfinement time is a discrete function as mentioned in Ref. [6]. We can find that $1/(mt_d)$ seems to approach
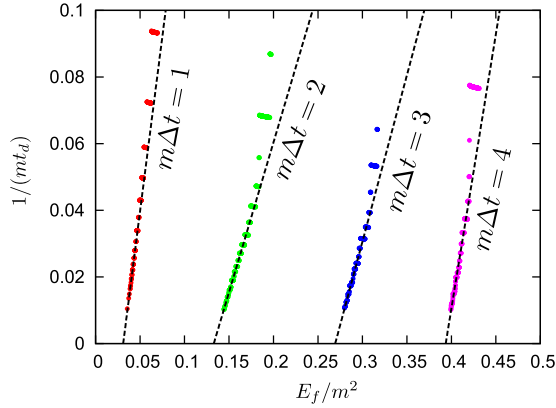
Fig. 11. Inverse of the deconfinement time t_d as a function of E_f. Blue, green, red and magentapoints correspond to numerical data for $m\Delta t = 1, 2, 3, 4$, respectively. Fitting line are shown by dashed lines. The points where the dashed lines and the horizontal axes intersect determine E_∞. (For interpretation of the references to color in this figure, the reader is referred to the web version of this article.)
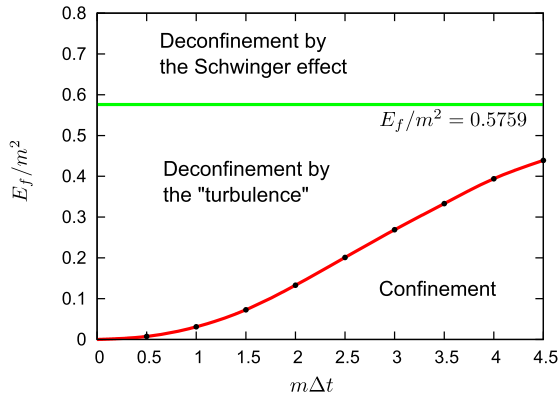

Fig. 12. Dynamical phase diagram for the electric field quench. (For interpretation of the references to color in this figure, the reader is referred to the web version of this article.)

the horizontal axis and touch there at non-zero E_f by extrapolating. Thus, the deconfinement time behaves as $t_d \sim 1/(E_f - E_\infty)$ as $E_f \to E_\infty \neq 0$. This indicates that the singularity formation does not occur for sufficiently small E_f. We fit the numerical data by linear functions and show them by dashed lines. From the fitting line, we estimate the lower bound of the singularity formation E_∞, at which the deconfinement time t_d will be infinite. In Fig. 12, we plot E_∞ for several Δt. Our numerical data are shown by black points. They are interpolated by a spline curve passing through the origin. This figure can be regarded as "dynamical phase diagram" for the electric field quench in supersymmetric QCD: (i) Below the red curve, we cannot observe the singularity formation. Thus, the system is in the confinement phase in this parameter region. (ii) Above the red curve and below the green curve, we find the naked singularity formation. Since the singularity formation implies the deconfinement, this region is regarded as a transient deconfinement phase. (iii) Above the green curve, we find the effective horizon on the D7-brane and the system settles down to a stationary phase eventually. This region can be regarded as the deconfinement phase induced by the Schwinger effect.
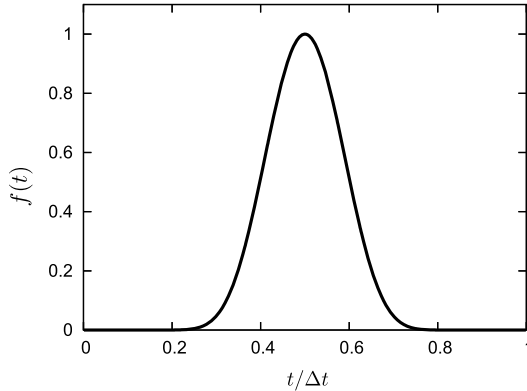
Fig. 13. Profile of the function $f(t)$ for $m = 1$.

5. Exploration of the essence of the turbulence

In the previous section, we have mentioned the turbulent meson condensation applying the quenched electric field. Now, the following questions arise: What is essential to the turbulent meson condensation? Does the worldvolume gauge field play an important role? If the electric field is present, the system has many elements suspected as a cause of the turbulence; two components of the fluctuations corresponding to the scalar and vector mesons, the mode mixing between those components in the existence of the static electric field (Stark effect), and so on. In this section, to answer these questions, we study time evolution of the D7-brane in the simplest set up: quark-mass quench.

5.1. Set up

We set the gauge potential to be zero and solve the dynamics of the D7-brane with time-dependent boundary condition as

$$W(t, \rho = \infty) = \mu(t) , \tag{31}$$

where, $\mu(t)$ corresponds to the time-dependent quark mass. In this case only the brane scalar fluctuations will be excited. We explicitly consider the following quark mass quench:

$$\mu(t) = m + \delta m \, f(t) , \quad f(t) \equiv \begin{cases} \exp\left[\frac{4}{m}\left(\frac{1}{t-\Delta t} - \frac{1}{t} + \frac{4}{\Delta t}\right)\right] & (0 < t < \Delta t) \\ 0 & \text{(otherwise)} . \end{cases} \tag{32}$$

The function $f(t)$ is a compactly supported C^∞ function whose maximum value is unity. The profile of the function is shown in Fig. 13. Therefore, the quench is characterized by two parameters Δt and δm, which means the quark mass increases by δm and then return to original value between the duration Δt.

Before the quench $t < 0$, we assume that the brane is static, that is, $W(t, \rho) = m$. For $t > 0$, the brane moves in $AdS_5 \times S^5$ because of the time dependence of the boundary condition. We solve the time evolution numerically. We follow the numerical method developed in Refs. [6,53].
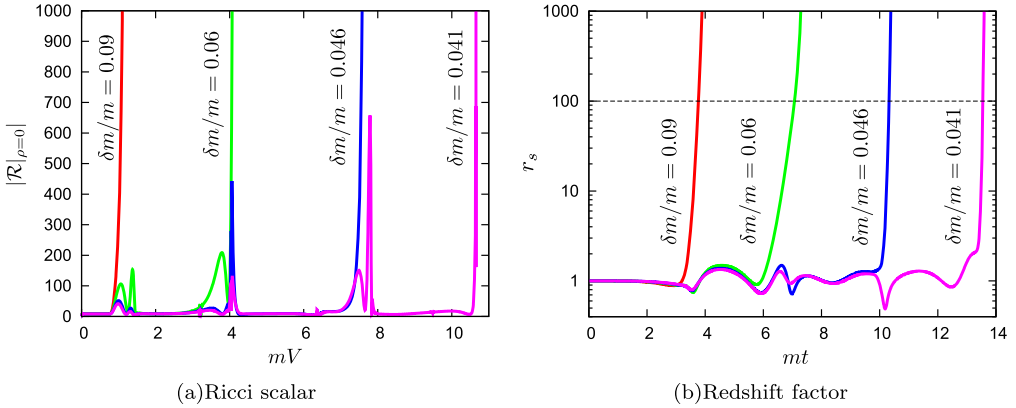
Fig. 14. (a) Ricci scalar estimated at the pole $\rho = 0$ against $V \equiv t - 1/r$. (b) Redshift factor against the boundary time t for $m\Delta t = 4$. In these figures, we fixed the time scale of the mass quench as $m\Delta t = 4$ and varied its amplitude as $\delta m/m = 0.09, 0.06, 0.046$ and 0.041.

5.2. Formation of a naked singularity

As the result of the numerical calculation, we found the similar behavior as the electric field quench: A pulse-like fluctuation induced by the mass quench propagates between the AdS boundary and the pole. After several bounces, the fluctuation collapses to a naked singularity depending on parameters δm and Δt. To see the singularity formation in the mass quench, we evaluate the Ricci scalar $\mathcal{R}$ with respect to the brane induced metric h_{ab}. In Fig. 14(a), we show the Ricci scalar monitored at $\rho = 0$ as a function of $V \equiv t - 1/r$. We can see that pulses are localized in several time intervals. This is because the pulse-like fluctuation induced by the mass quench propagates between the AdS boundary and the pole. When the pulse arrive at the pole, the brane is strongly bended and the scalar curvature has large value. We can find that the Ricci scalar diverges at several places depending on the amplitude of the mass quench. The pulse is getting sharp as time increases and, eventually, it collapse to a naked singularity. For example, for $\delta m/m = 0.046$, the scalar curvature diverges when the pulse comes to the pole for the third time. This means that, even if there is no gauge field on the D7-brane, a naked singularity can be created by the dynamical process.

5.3. Deconfinement time

Following Ref. [6], we study the deconfinement time. In Fig. 14(b), we show the redshift factor as the function of the boundary time t. The redshift factor suddenly increases around the retarded time at which the singularity is formed. As a result, it exceeds the criterion of the deconfinement $r_s = 100$ and eventually, it diverges. In Fig. 15, the deconfinement time t_d is shown as a function of δm. We can see that the t_d is a discrete function of δm like the electric field quench. This is because the number of bounces needed for the singularity formation depends on the δm as shown in the previous subsection.

Now, we check if the turbulent behavior can occur for arbitrary small δm. Following the case of the electric field quench, we focus on the inverse of the deconfinement time. In Fig. 16, we plot $1/(mt_d)$ against $\delta m/m$ for $m\Delta t = 2, 3, 4$. Our numerical data are shown by the points in the figure. We fit the numerical data by a second order polynomial $a\delta m^2 + b\delta m + c$. The fitting curves
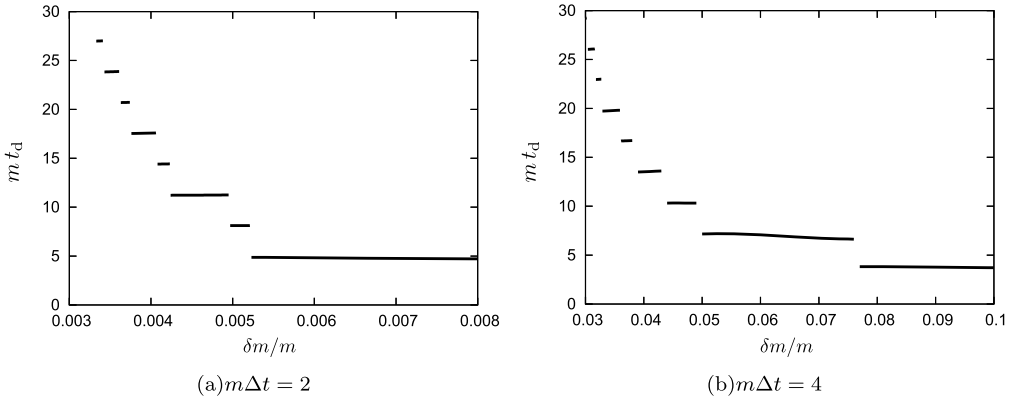
Fig. 15. Deconfinement times t_d against δm for $m\Delta t = 2, 4$. They are given by discrete functions of δm.
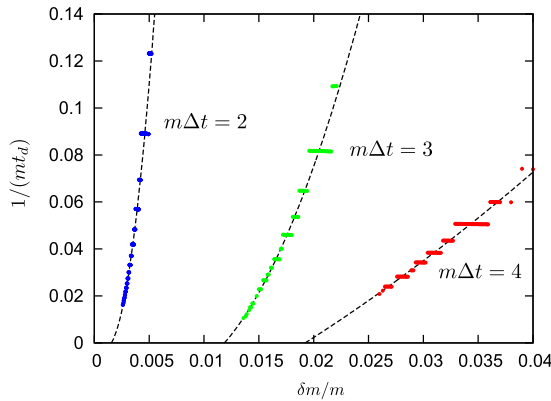

Fig. 16. Reciprocal for the deconfinement time t_d as a function of δm. Blue, green and red points correspond to numerical data for $m\Delta t = 2, 3, 4$, respectively. Fitting curves are shown by dashed curves. (For interpretation of the references to color in this figure, the reader is referred to the web version of this article.)

are shown by dashed curves in the figure. The dashed curves intersect with the horizontal axis. Thus, the deconfinement time behaves as $t_d \sim 1/(\delta m - \delta m_\infty)$ as $\delta m \to \delta m_\infty \neq 0$. The critical value of δm at which the deconfinement time will be infinite can be estimated as $\delta m_\infty/m = 0.0016, 0.0119, 0.0192$ for $m\Delta t = 2, 3, 4$, respectively. We find that they are non-zero value. This indicates that the singularity formation does not occur for sufficiently small perturbations.

5.4. Meson turbulence in mass quench

In order to perform spectral analysis, we decompose the non-linear solution $w(t, z) = W(t, z) - m$ obtained numerically into the meson eigen-modes $e_n(z)$ around the supersymmetric background. Setting parameters as $\delta m/m = 0.031$ and $m\Delta t = 4$, in Fig. 17, we plot the spectrum for several time slices, $mt = 8, 16$, and 22.8, while the time $mt = 22.8$ is just before deconfinement. For the mass quench, the energy spectrum in linear theory computed from Eq. (26) is given by
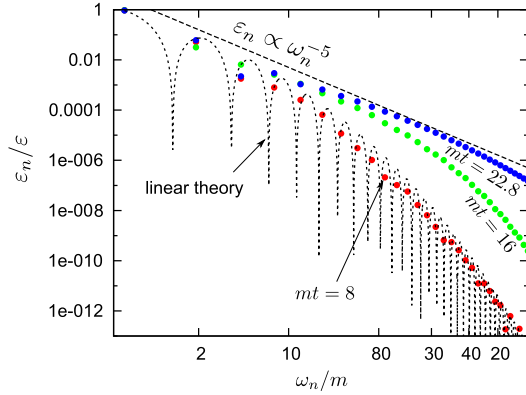
Fig. 17. Energy spectrum for several time slices, $mt = 8, 16, 22.8$. Parameters as $\delta m/m = 0.031$ and $m\Delta t = 4$. It is given by the linear theory at first, and then seems to approach $\varepsilon_n \propto \omega_n^{-5}$ as time increases.

$$\varepsilon_n^{\text{linear}} = 4\pi^2 m \omega_n^2 \sqrt{\omega_n^2 + m^2} \, \delta m^2 |\hat{f}(\omega_n)|^2, \tag{33}$$

where we have used $\hat{\chi}_0(\omega) = \delta m \hat{f}(\omega)$ and $\hat{f}(\omega) = (2\pi)^{-1} \int_{-\infty}^{\infty} f(t) e^{-i\omega t} dt$. We also show the spectrum in the figure regarding ω_n as a continuous number. We can see that the energy spectrum $\varepsilon_n/\varepsilon$ is given by the linear theory at first, and then evolving with energy flow from low to high frequency modes because of non-linearity. This means that, even though the worldvolume gauge field dose not exist, the turbulent meson condensation can arise from the brane fluctuations $w(t, z)$ only. We also see that the energy spectrum seems to approach $\varepsilon_n \propto \omega_n^{-5}$ just before the deconfinement in the quark mass quench as well as the electric field quench. This implies that Kolmogorov-like scaling $\varepsilon_n \propto \omega_n^{-5}$ is universal for the deconfinement in $\mathcal{N} = 2$ supersymmetric QCD.

5.5. Essence of the turbulence

The results shown in the previous and this sections lead us the following conclusions. The worldvolume gauge field or the quench induced by the electric field is not indispensable for the probe-brane turbulence. In addition, although the existence of the static electric filed causes the mass shift of the spectrum and also the mode mixing between the scalar and the vector mesons, it does not spoil the turbulence.

Since the initial energy spectrum excited by the quenches can be determined by the linear theory, non-linearity has not been so significant to excite the brane. It means that perturbative (not infinitesimal but finite) inputs are enough for the turbulence on the brane. The non-linearity plays an important role in the evolution with energy transfer to higher meson modes after the brane is excited.

Here, we point out the relation with the present result and the "weak turbulence theory" developed in plasma physics [51,52]. When the electric field is switched on or the quark mass changes, the meson modes are excited, and their dynamics is described by the time evolution of mode coefficients $c_n(t)$. At lowest order, the meson modes obey a kinetic equation

$$\frac{d\tilde{c}_n(t)}{dt} = \sum_{n,n',n''} W_{nn'n''} \tilde{c}_{n'}(t) \tilde{c}_{n''}(t) + \cdots, \tag{34}$$

where the coupling constant $W_{nn'n''}$ represents 3-meson interaction that is generically present in the effective meson Lagrangian. One can obtain the coupling by expanding the D7-brane action [13], and the kinetic equation can be obtained as an equation of motion derived from the effective Lagrangian (after a suitable redefinition of the meson fields[3]). Energy conservation is weakly enforced in $W_{nn'n''}$, i.e., $\omega_n \sim \omega_{n'} + \omega_{n''}$, where the excess energy is absorbed by other degrees of freedom. Eq. (34) is nothing but the canonical model for weak turbulence [52] and describes how the excitation spreads out among the meson modes. Before the quenches, the mesons are not excited ($c_n(-\infty) = 0$). Cranking up the field, the modes are excited as the linear theory predicts (26), while the coupling constant $W_{nn'n''}(t)$ is also modified since the electric field changes the properties of the mesons. If the final field strength is small, the change of $W_{nn'n''}$ is not significant. The time evolution of the meson modes and how the energy is transfered to higher energies are described by the kinetic equation (34). The power law distribution we find in Figs. 10(b) and 17 implies a scaling behavior for the coupling constant. It is an interesting future problem to explain this from the generic properties of the effective meson theory, which will prove the universality of the meson turbulence phenomenon.

Although our numerical calculations have been performed only for several variations of the quenches characterized by specific functions, a functional form of the quench can always be mapped to an initial energy spectrum by the linear theory. Thus, we need to discuss the inevitability of the meson turbulence by the initial spectrum, not by the quench function itself. This implies that anything which can excite the brane will be a trigger of the turbulence. Once an initial spectrum is given, the energy distribution evolves according to the kinetic equation of weak turbulence (34), and under a certain kind of scaling property for the coupling W the system is expected generically to flow to a turbulence-like power law. Indeed, if we change the mass of the black hole in the bulk by the method in Ref. [53], namely temperature quench, we can confirm occurrence of the meson turbulence. It is expected that the turbulence can universally occur for wider systems of fluctuations of the probe branes.

6. Summary

In this paper, we have demonstrated in $\mathcal{N} = 2$ supersymmetric QCD with large N_c and strong coupling limit, that a meson turbulence is universal at quark deconfinement, by using the AdS/CFT correspondence. The "meson turbulence" is defined as a power-law distribution of the energy ε_n for the n-th meson resonance with mass ω_n,

$$\varepsilon_n \propto (\omega_n)^\alpha \tag{35}$$

with a certain negative parameter α which is unique to the theory. We have studied various ways to produce the quark deconfinement; (1) static electric field, (2) electric field quench, and (3) mass quench. For (2) and (3), we can choose various sets of external parameters such as the final value of the electric field and the duration of the change of the electric field. Analyses in all the cases lead to a universal power

$$\alpha = -5 \tag{36}$$

---

[3] Free mesons oscillate with a trivial phase factor with the mass ω_n, since the free equation of motion for the homogeneous meson is $(\partial_t^2 + \omega_n^2)c_n(t) = 0$. To get rid of this phase factor, we need to redefine $c_n(t) \equiv b_n(t) \exp[i\omega_n t]$. Then this free $b_n(t)$ obeys the equation $(\partial_t^2 + 2i\omega_n \partial_t)b_n(t) = 0$, so we further redefine $(\partial_t + 2i\omega_n)b_n(t) \equiv \tilde{c}_n(t)$ such that the free equation of motion is $\partial_t \tilde{c}_n(t) = 0$. The weak turbulence equation (34) uses this eigenbasis.

for the $\mathcal{N} = 2$ supersymmetric QCD. This surprising universality of the turbulent meson condensation suggests that any QCD-like theory may have its own α at quark deconfinement caused by any means.

As we have described in the introduction, normally one expects that the energy storage for mass ω_n meson should be $\sim \exp[-\omega_n/T]$ where T is a finite temperature. QCD-string theory suggests that this exponentially suppressed behavior turns to a power-law near the critical point of the phase transition. We have confirmed this change to the power-law in our AdS/CFT calculation of the quarks deconfinement.

Our finding (35) is a kind of weak turbulence (energy cascade from low momenta to higher momenta), if we see the meson mass ω_n as a momentum. Indeed, the meson mass is a momentum in the holographic direction in AdS/CFT correspondence. So our energy distribution is a turbulence in holographic space, so may be called as a "holographic turbulence".

In the course of investigating the conditions for the quark deconfinement, we found an interesting "dynamical phase diagram" of the $\mathcal{N} = 2$ supersymmetric QCD, see Fig. 12. The standard case with static electric field corresponds to the right edge of the diagram (that is $\Delta t = \infty$, *i.e.* adiabatic limit), where there exists a clear critical value $E_{\text{Schwinger}}$ (the green line) below which we have the confined phase. However in the time-dependent case we found that the deconfinement line is lowered significantly. In particular, when the quench becomes more abrupt, the final value of the electric field can be smaller for the deconfinement to occur. We worked at the supersymmetric QCD at large N_c limit and the theory is different from QCD, but our result is quite suggestive to heavy ion experiments at which we know there are time-dependent electric field — even though the magnitude of the electric field is small compared to the QCD scale, if the time-dependence is abrupt enough, the electric field can help the deconfinement to occur.

However, the large N_c limit would be very important for our meson turbulence. The higher resonant states in reality have broader widths, and only at the large N_c limit we can clearly see the resonances. In fact, the nearly-free QCD-string picture is a good picture at large N_c, as the sting interaction such as joining-splitting and reconnection is measures in the unit of $1/N_c$. In reality with $N_c = 3$, longer strings are not favored and strings tend to break. Nevertheless, we hope that the analyses at large N_c can provide at least an alternative and interesting picture of quark confinement/deconfinement.

Acknowledgements

References

[1] K. Hashimoto, S. Kinoshita, K. Murata, T. Oka, Turbulent meson condensation in quark deconfinement, arXiv: 1408.6293 [hep-th].

[2] J.M. Maldacena, The large N limit of superconformal field theories and supergravity, Adv. Theor. Math. Phys. 2 (1998) 231, arXiv:hep-th/9711200.

[3] S. Gubser, I.R. Klebanov, A.M. Polyakov, Gauge theory correlators from noncritical string theory, Phys. Lett. B 428 (1998) 105.

[4] E. Witten, Anti-de Sitter space and holography, Adv. Theor. Math. Phys. 2 (1998) 253.

[5] A. Karch, E. Katz, Adding flavor to AdS / CFT, J. High Energy Phys. 0206 (2002) 043, arXiv:hep-th/0205236.

[6] K. Hashimoto, S. Kinoshita, K. Murata, T. Oka, J. High Energy Phys. 1409 (2014) 126, arXiv:1407.0798 [hep-th].

[7] A.M. Polyakov, Thermal properties of gauge fields and quark liberation, Phys. Lett. B 72 (1978) 477.

[8] B. Lucini, M. Teper, U. Wenger, Properties of the deconfining phase transition in SU(N) gauge theories, J. High Energy Phys. 0502 (2005) 033, arXiv:hep-lat/0502003.

[9] M. Hanada, J. Maltz, L. Susskind, Deconfinement transition as black hole formation by the condensation of QCD strings, arXiv:1405.1732 [hep-th].

[10] R.D. Pisarski, O. Alvarez, Strings at finite temperature and deconfinement, Phys. Rev. D 26 (1982) 3735.

[11] A. Patel, A flux tube model of the finite temperature deconfining transition in QCD, Nucl. Phys. B 243 (1984) 411.

[12] P. Bizon, A. Rostworowski, On weakly turbulent instability of anti-de Sitter space, Phys. Rev. Lett. 107 (2011) 031102, arXiv:1104.3702 [gr-qc].

[13] M. Kruczenski, D. Mateos, R.C. Myers, D.J. Winters, Meson spectroscopy in AdS/CFT with flavor, J. High Energy Phys. 0307 (2003) 049, arXiv:hep-th/0304032.

[14] P.B. Arnold, G.D. Moore, QCD plasma instabilities: the non-Abelian cascade, Phys. Rev. D 73 (2006) 025006, arXiv:hep-ph/0509206.

[15] P.B. Arnold, G.D. Moore, The turbulent spectrum created by non-Abelian plasma instabilities, Phys. Rev. D 73 (2006) 025013, arXiv:hep-ph/0509226.

[16] A.H. Mueller, A.I. Shoshi, S.M.H. Wong, On Kolmogorov wave turbulence in QCD, Nucl. Phys. B 760 (2007) 145, arXiv:hep-ph/0607136.

[17] P.B. Arnold, G.D. Moore, Non-Abelian plasma instabilities for extreme anisotropy, Phys. Rev. D 76 (2007) 045009, arXiv:0706.0490 [hep-ph].

[18] A. Rebhan, M. Strickland, M. Attems, Instabilities of an anisotropically expanding non-Abelian plasma: 1D + 3V discretized hard-loop simulations, Phys. Rev. D 78 (2008) 045023, arXiv:0802.1714 [hep-ph].

[19] J. Berges, S. Scheffler, D. Sexty, Turbulence in nonabelian gauge theory, Phys. Lett. B 681 (2009) 362, arXiv:0811.4293 [hep-ph].

[20] K. Dusling, T. Epelbaum, F. Gelis, R. Venugopalan, Role of quantum fluctuations in a system with strong fields: onset of hydrodynamical flow, Nucl. Phys. A 850 (2011) 69, arXiv:1009.4363 [hep-ph].

[21] M.E. Carrington, A. Rebhan, Perturbative and nonperturbative Kolmogorov turbulence in a gluon plasma, Eur. Phys. J. C 71 (2011) 1787, arXiv:1011.0393 [hep-ph].

[22] J.P. Blaizot, F. Gelis, J.F. Liao, L. McLerran, R. Venugopalan, Bose–Einstein condensation and thermalization of the quark gluon plasma, Nucl. Phys. A 873 (2012) 68, arXiv:1107.5296 [hep-ph].

[23] S. Floerchinger, U.A. Wiedemann, Fluctuations around Bjorken flow and the onset of turbulent phenomena, J. High Energy Phys. 1111 (2011) 100, arXiv:1108.5535 [nucl-th].

[24] K. Fukushima, Evolving glasma and Kolmogorov spectrum, Acta Phys. Pol. B 42 (2011) 2697, arXiv:1111.1025 [hep-ph].

[25] K. Fukushima, Turbulent pattern formation and diffusion in the early-time dynamics in relativistic heavy-ion collisions, Phys. Rev. C 89 (2) (2014) 024907, arXiv:1307.1046 [hep-ph].

[26] R. Micha, I.I. Tkachev, Relativistic turbulence: a long way from preheating to equilibrium, Phys. Rev. Lett. 90 (2003) 121301, arXiv:hep-ph/0210202.

[27] R. Micha, I.I. Tkachev, Turbulent thermalization, Phys. Rev. D 70 (2004) 043538, arXiv:hep-ph/0403101.

[28] J. Berges, A. Rothkopf, J. Schmidt, Non-thermal fixed points: effective weak-coupling for strongly correlated systems far from equilibrium, Phys. Rev. Lett. 101 (2008) 041603, arXiv:0803.0131 [hep-ph].

[29] J. Berges, G. Hoffmeister, Nonthermal fixed points and the functional renormalization group, Nucl. Phys. B 813 (2009) 383, arXiv:0809.5208 [hep-ph].

[30] J. Berges, D. Sexty, Strong versus weak wave-turbulence in relativistic field theory, Phys. Rev. D 83 (2011) 085004, arXiv:1012.5944 [hep-ph].

[31] J. Berges, D. Sexty, Bose condensation far from equilibrium, Phys. Rev. Lett. 108 (2012) 161601, arXiv:1201.0687 [hep-ph].

[32] J. Berges, S. Schlichting, D. Sexty, Over-populated gauge fields on the lattice, Phys. Rev. D 86 (2012) 074006, arXiv:1203.4646 [hep-ph].

[33] S. Schlichting, Turbulent thermalization of weakly coupled non-abelian plasmas, Phys. Rev. D 86 (2012) 065008, arXiv:1207.1450 [hep-ph].

[34] J. Berges, K. Boguslavski, S. Schlichting, R. Venugopalan, Universal attractor in a highly occupied non-Abelian plasma, Phys. Rev. D 89 (2014) 114007, arXiv:1311.3005 [hep-ph].

[35] J. Berges, D. Gelfand, S. Scheffler, D. Sexty, Simulating plasma instabilities in SU(3) gauge theory, Phys. Lett. B 677 (2009) 210, arXiv:0812.3859 [hep-ph].

[36] A. Karch, A. O'Bannon, Metallic AdS/CFT, J. High Energy Phys. 0709 (2007) 024, arXiv:0705.3870 [hep-th].

[37] T. Albash, V.G. Filev, C.V. Johnson, A. Kundu, Quarks in an external electric field in finite temperature large N gauge theory, J. High Energy Phys. 0808 (2008) 092, arXiv:0709.1554 [hep-th].

[38] J. Erdmenger, R. Meyer, J.P. Shock, AdS/CFT with flavour in electric and magnetic Kalb–Ramond fields, J. High Energy Phys. 0712 (2007) 091, arXiv:0709.1551 [hep-th].

[39] J.J. Atick, E. Witten, The hagedorn transition and the number of degrees of freedom of string theory, Nucl. Phys. B 310 (1988) 291.

[40] R. Hagedorn, Statistical thermodynamics of strong interactions at high-energies, Suppl. Nuovo Cim. 3 (1965) 147.

[41] Y. Sato, K. Yoshida, Holographic description of the Schwinger effect in electric and magnetic fields, J. High Energy Phys. 1304 (2013) 111, arXiv:1303.0112 [hep-th].

[42] Y. Sato, K. Yoshida, Universal aspects of holographic Schwinger effect in general backgrounds, J. High Energy Phys. 1312 (2013) 051, arXiv:1309.4629 [hep-th].

[43] K. Hashimoto, T. Oka, A. Sonoda, Electromagnetic instability in holographic QCD, arXiv:1412.4254 [hep-th], J. High Energy Phys. (2015), in press.

[44] K. Hashimoto, D.E. Kharzeev, Entropic destruction of heavy quarkonium in non-Abelian plasma from holography, arXiv:1411.0618 [hep-th].

[45] R. Emparan, Remarks on the Atick–Witten behavior and strings near black hole horizons, arXiv:hep-th/9412003.

[46] O. Bergman, K. Hori, P. Yi, Confinement on the brane, Nucl. Phys. B 580 (2000) 289, arXiv:hep-th/0002223.

[47] G.W. Gibbons, K. Hori, P. Yi, String fluid from unstable D-branes, Nucl. Phys. B 596 (2001) 136, arXiv:hep-th/0009061.

[48] G. Gibbons, K. Hashimoto, P. Yi, Tachyon condensates, Carrollian contraction of Lorentz group, and fundamental strings, J. High Energy Phys. 0209 (2002) 061, arXiv:hep-th/0209034.

[49] D. Mateos, P.K. Townsend, Supertubes, Phys. Rev. Lett. 87 (2001) 011602, arXiv:hep-th/0103030.

[50] H.P. de Oliveira, L.A. Pando Zayas, E.L. Rodrigues, A Kolmogorov–Zakharov spectrum in AdS gravitational collapse, Phys. Rev. Lett. 111 (5) (2013) 051101, arXiv:1209.2369 [hep-th].

[51] R.Z. Sagdeev, A.A. Galeev, Nonlinear Plasma Theory, Benjamin, New York, 1969.

[52] B. Coppi, M.N. Rosenbluth, R.N. Sudan, Ann. Phys. 55 (1969) 207.

[53] T. Ishii, S. Kinoshita, K. Murata, N. Tanahashi, Dynamical meson melting in holography, J. High Energy Phys. 1404 (2014) 099, arXiv:1401.5106 [hep-th].